

A STUDY ON EFFECT OF STIFFENER GEOMETRY ON THE MODAL FREQUENCIES OF A ROTATING DISK WITH RADIAL STIFFENERS USING FEM AND ANALYTICAL METHODS

Subhrajit Bhattacharya [†]

Third year student, Department of Mechanical Engineering, IIT Kharagpur, INDIA.
Email: subhrajit83@yahoo.co.in , subhrajit_02@mech.iitkgp.ernet.in

ABSTRACT

The present work deals with the problem of increasing the natural frequencies and hence the critical speeds of a rotating disk by inserting thin radial stiffeners into the disk. Introduction of such stiffeners of higher strength and rigidity though does not affect the properties and performance of the disk reasonably, according to the present analysis it is found that they can successfully increase the natural frequencies of the disk, both in static as well as rotating conditions.

Using the FEM software Ansys 8.0, modal analyses of the rotating annular disk with radial stiffeners of different geometries were performed. A gradual development of the stiffener geometry on the basis of conclusions drawn from intermediate results finally yielded a stiffener, which could successfully push up the modal frequencies, and hence potentially increase the critical speeds of the disk.

In an analytical approach to the problem, though it was rather difficult to incorporate the stiffener geometry, some elementary analyses were performed and after a thorough mathematical investigation, a partial differential equation was set to describe the vibration of the disk with stiffeners. However a final analytical solution could not be achieved at the present moment due to the complexity of the equation.

INTRODUCTION

Rotating disks and similar rotating objects appear in various practical problems in classical engineering applications like rotating shafts, disk clutches, cams & turbine blades. Moreover, in many important recent applications like rotating data storage devices in computers, the disks generally have to undergo extreme conditions of stresses at extremely high rotation speeds assuming orders of few thousand rotations per minutes. The problem takes critical turn when the frequency of rotation of the disk matches with its natural frequencies of vibration. Hence an investigation into the problem seeking ways for stiffening the disk without altering much of its dimensions & material properties and still result in an increase in such critical frequency is highly desirable.

[†] Postal address for correspondence: 53/1, Canal Street, Kolkata-700048, INDIA.
Phone number: 91-033-25214513

PRESENT ANALYSIS – THE ANALYTICAL APPROACH

In the present analysis we deal with only the out of plane modes of vibration of the plate/disk. Hence we have only one displacement variable, w , which denotes the displacement of a point on the disk along the axial direction from its un-displaced position. Here w is a function of r , θ and t , where r & θ are the space variables in cylindrical polar coordinates and t is the time. As we are interested in finding out the natural modes of vibration, we assume that w is a simple harmonic function of time with the same frequency and phase but varying amplitudes for all the points on the disk. That is,

$$w(r, \theta, t) = u(r, \theta) \cdot e^{i\omega_n t} \quad (2)$$

where, ω_n is the frequency of the particular natural mode of vibration.

Moments on an elemental portion of the disk. We start with the expression for bending and twisting moments on an element of the disk. The expressions for moments per unit length have been given by Timoshenko [1] for any orthogonal coordinate system. We have used the expression for cylindrical polar coordinates. Bending moments per unit length are given by,

$$M_r = D \left(\frac{1}{\rho_\theta} + \frac{\nu}{\rho_r} \right) \quad (3)$$

$$M_\theta = -D \left(\frac{1}{\rho_r} + \frac{\nu}{\rho_\theta} \right) \quad (4)$$

where, ρ_r and ρ_θ are the radii of curvature along a radial line and tangent respectively,

$$\rho_r = -\frac{1}{\frac{\partial^2 w}{\partial r^2}} \quad \text{and} \quad \rho_\theta = -\frac{1}{\frac{1}{r} \frac{\partial w}{\partial r} + \frac{1}{r^2} \frac{\partial^2 w}{\partial \theta^2}}$$

And the twisting moment per unit length is given by,

$$M_{\theta r} = D(1-\nu) \left[\frac{1}{r} \frac{\partial^2 w}{\partial r \partial \theta} - \frac{1}{r^2} \frac{\partial w}{\partial \theta} \right] \quad (5)$$

$$\text{and, } M_{r\theta} = -M_{\theta r}$$

Here it may be noted that E , ν , and hence D are functions of r and θ .

The following figure shows the moment vectors due to the above acting on an elemental portion of the disk. It may be noted here that the notations used by Timoshenko for M_r and M_θ have been interchanged in the present analysis.

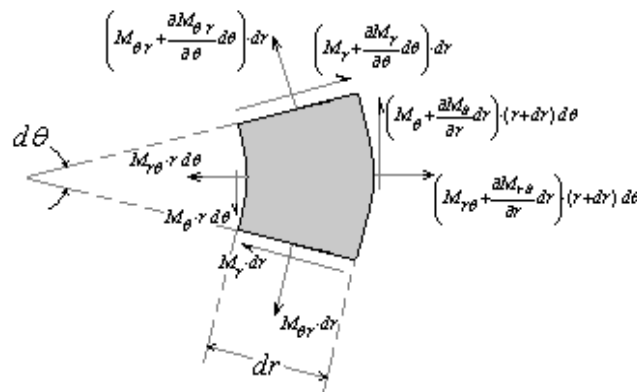


fig - 1

Shear stresses. Now, figure 2 shows the direction of the shear stresses acting on the element which contribute to the moments along e_r and e_θ directions.

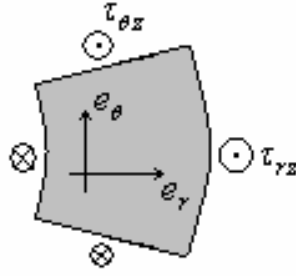


fig - 2

As the moment of inertia of the element about any axis (e_r or e_θ) embedded on it is a differential of order 4, the rotation of the element about the axes can be neglected. Hence we consider equilibrium of the bending & twisting moments and the moments due to the shear forces on the element.

Considering moment about e_r ,

$$\frac{\partial(rM_{r\theta})}{\partial r} dr d\theta + \frac{\partial M_r}{\partial \theta} dr d\theta - M_\theta dr d\theta + \tau_{\theta z} h dr \cdot r d\theta = 0$$

$$\therefore \tau_{\theta z} = -\frac{1}{hr} \left[\frac{\partial M_r}{\partial \theta} + r \frac{\partial M_{r\theta}}{\partial r} + M_{r\theta} - M_\theta \right] \quad (6)$$

And, considering moment about e_θ ,

$$\frac{\partial(rM_\theta)}{\partial r} dr d\theta + \frac{\partial M_\theta}{\partial \theta} dr d\theta + M_r dr d\theta - \tau_{rz} h r d\theta dr = 0$$

$$\therefore \tau_{rz} = \frac{1}{hr} \left[\frac{\partial M_\theta}{\partial \theta} + r \frac{\partial M_\theta}{\partial r} + M_r + M_\theta \right] \quad (7)$$

Components of Radial and Circumferential stresses due to rotation of the disk. If we consider the disk to be pre-stressed, there will be normal stresses along e_r and e_θ . As the element has a curvature both along e_r and e_θ directions, there will be components of forces due to σ_r and σ_θ along e_z (figure 3).

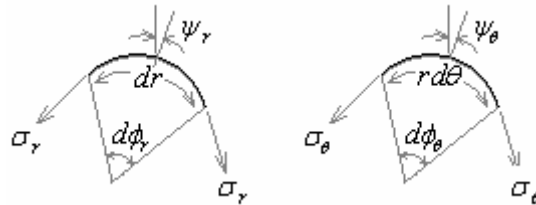


fig - 3

On performing a simple analysis, it can be shown that the components of the forces due to radial and circumferential stresses along $-e_z$ are respectively given by,

$$F_{\sigma_r} = (\sigma_r r d\theta \cdot h) \cdot d\phi_r \cdot \cos(\psi_r) = \sigma_r r d\theta \cdot h \frac{dr}{\rho_r} \cos(\psi_r) \quad (8)$$

$$\text{and, } F_{\sigma_\theta} = (\sigma_\theta dr h) \cdot d\phi_\theta \cdot \cos(\psi_\theta) = \sigma_\theta dr h \frac{r d\theta}{\rho_\theta} \cos(\psi_\theta) \quad (9)$$

$$\text{where, } \psi_r = \tan^{-1}\left(\frac{\partial w}{\partial r}\right) \text{ and } \psi_\theta = \tan^{-1}\left(\frac{1}{r} \frac{\partial w}{\partial \theta}\right).$$

For a disk with r_i and r_o as internal and external radii respectively and fixed at the inner circumference (as in the present case) and rotating with angular frequency ω , the radial and circumferential stresses are given by,

$$\sigma_r = \frac{3+\nu}{8} \rho \omega^2 \left(r_i^2 + r_o^2 - \frac{r_i^2 + r_o^2}{r^2} - r^2 \right) \quad (11)$$

$$\text{and, } \sigma_\theta = \frac{3+\nu}{8} \rho \omega^2 \left(r_i^2 + r_o^2 + \frac{r_i^2 + r_o^2}{r^2} - \frac{1+3\nu}{3+\nu} r^2 \right) \quad (12)$$

The final equation of motion. Hence, the net force on the element along e_z due to the τ_{rz} , $\tau_{\theta z}$, σ_r and σ_θ causes it to accelerate along e_z . Hence, the final equation of motion is given by,

$$\rho h dr \cdot r d\theta \frac{\partial^2 w}{\partial t^2} = \frac{\partial}{\partial \theta} (\tau_{\theta z} h dr) d\theta + \frac{\partial}{\partial r} (\tau_{rz} h \cdot r d\theta) dr - F_{\sigma_r} - F_{\sigma_\theta}$$

where, ρ is the density of the material and is a function of r and θ .

This gives,

$$\frac{\partial^2 w}{\partial t^2} = \frac{1}{\rho r} \left[\frac{\partial \tau_{\theta z}}{\partial \theta} + r \frac{\partial \tau_{rz}}{\partial r} + \tau_{rz} - \frac{r \sigma_r}{\rho_r} \frac{1}{\sqrt{1 + \left(\frac{\partial w}{\partial r}\right)^2}} - \frac{r \sigma_\theta}{\rho_\theta} \frac{1}{\sqrt{1 + \left(\frac{1}{r} \frac{\partial w}{\partial \theta}\right)^2}} \right] \quad (10)$$

Now, putting in (10) the expression for w in terms of u and ω_n from (2), and performing all the calculations and simplifications using Mathematica 5.1 the following differential equation was obtained,

$$\begin{aligned} -\rho r \omega_n^2 u = & \frac{1}{8} \left[\frac{r^3 \omega^2 \rho[x, \theta] \sqrt{1 + \frac{u^{(0,1)}[x, \theta]^2}{r^2}} u^{(0,2)}[x, \theta]}{r^2 + u^{(0,1)}[x, \theta]^2} + \frac{3 r r i^2 \omega^2 \rho[x, \theta] \sqrt{1 + \frac{u^{(0,1)}[x, \theta]^2}{r^2}} u^{(0,2)}[x, \theta]}{r^2 + u^{(0,1)}[x, \theta]^2} \right. \\ & \frac{3 r r o^2 \omega^2 \rho[x, \theta] \sqrt{1 + \frac{u^{(0,1)}[x, \theta]^2}{r^2}} u^{(0,2)}[x, \theta]}{r^2 + u^{(0,1)}[x, \theta]^2} - \frac{3 r^3 \omega^2 \nu[x, \theta] \rho[x, \theta] \sqrt{1 + \frac{u^{(0,1)}[x, \theta]^2}{r^2}} u^{(0,2)}[x, \theta]}{r^2 + u^{(0,1)}[x, \theta]^2} \\ & \frac{r r i^2 \omega^2 \nu[x, \theta] \rho[x, \theta] \sqrt{1 + \frac{u^{(0,1)}[x, \theta]^2}{r^2}} u^{(0,2)}[x, \theta]}{r^2 + u^{(0,1)}[x, \theta]^2} + \frac{r r o^2 \omega^2 \nu[x, \theta] \rho[x, \theta] \sqrt{1 + \frac{u^{(0,1)}[x, \theta]^2}{r^2}} u^{(0,2)}[x, \theta]}{r^2 + u^{(0,1)}[x, \theta]^2} \\ & \frac{3 r i^2 \omega^2 \rho[x, \theta] \sqrt{\frac{r^2 + u^{(0,1)}[x, \theta]^2}{r^2}} u^{(0,2)}[x, \theta]}{r^3 + r u^{(0,1)}[x, \theta]^2} + \frac{3 r o^2 \omega^2 \rho[x, \theta] \sqrt{\frac{r^2 + u^{(0,1)}[x, \theta]^2}{r^2}} u^{(0,2)}[x, \theta]}{r^3 + r u^{(0,1)}[x, \theta]^2} \\ & \frac{r i^2 \omega^2 \nu[x, \theta] \rho[x, \theta] \sqrt{\frac{r^2 + u^{(0,1)}[x, \theta]^2}{r^2}} u^{(0,2)}[x, \theta]}{r^3 + r u^{(0,1)}[x, \theta]^2} + \frac{r o^2 \omega^2 \nu[x, \theta] \rho[x, \theta] \sqrt{\frac{r^2 + u^{(0,1)}[x, \theta]^2}{r^2}} u^{(0,2)}[x, \theta]}{r^3 + r u^{(0,1)}[x, \theta]^2} \\ & \left. \frac{8 e d^{(0,2)}[x, \theta] u^{(0,2)}[x, \theta]}{h r^3} + \frac{16 u^{(0,1)}[x, \theta] \nu^{(0,1)}[x, \theta] e d^{(1,0)}[x, \theta]}{h r^2} - \frac{24 u^{(0,2)}[x, \theta] e d^{(1,0)}[x, \theta]}{h r^2} \right] \end{aligned}$$

$$\begin{aligned}
& \frac{x^4 \omega^2 \rho[x, \theta] \sqrt{1 + \frac{u^{(0,1)}[x, \theta]^2}{x^2}} u^{(1,0)}[x, \theta]}{x^2 + u^{(0,1)}[x, \theta]^2} + \frac{3 x i^2 \omega^2 \rho[x, \theta] \sqrt{1 + \frac{u^{(0,1)}[x, \theta]^2}{x^2}} u^{(1,0)}[x, \theta]}{x^2 + u^{(0,1)}[x, \theta]^2} \\
& \frac{3 x^2 x i^2 \omega^2 \rho[x, \theta] \sqrt{1 + \frac{u^{(0,1)}[x, \theta]^2}{x^2}} u^{(1,0)}[x, \theta]}{x^2 + u^{(0,1)}[x, \theta]^2} + \frac{3 x o^2 \omega^2 \rho[x, \theta] \sqrt{1 + \frac{u^{(0,1)}[x, \theta]^2}{x^2}} u^{(1,0)}[x, \theta]}{x^2 + u^{(0,1)}[x, \theta]^2} \\
& \frac{3 x^2 x o^2 \omega^2 \rho[x, \theta] \sqrt{1 + \frac{u^{(0,1)}[x, \theta]^2}{x^2}} u^{(1,0)}[x, \theta]}{x^2 + u^{(0,1)}[x, \theta]^2} - \frac{3 x^4 \omega^2 v[x, \theta] \rho[x, \theta] \sqrt{1 + \frac{u^{(0,1)}[x, \theta]^2}{x^2}} u^{(1,0)}[x, \theta]}{x^2 + u^{(0,1)}[x, \theta]^2} \\
& \frac{x i^2 \omega^2 v[x, \theta] \rho[x, \theta] \sqrt{1 + \frac{u^{(0,1)}[x, \theta]^2}{x^2}} u^{(1,0)}[x, \theta]}{x^2 + u^{(0,1)}[x, \theta]^2} + \frac{x^2 x i^2 \omega^2 v[x, \theta] \rho[x, \theta] \sqrt{1 + \frac{u^{(0,1)}[x, \theta]^2}{x^2}} u^{(1,0)}[x, \theta]}{x^2 + u^{(0,1)}[x, \theta]^2} \\
& \frac{x o^2 \omega^2 v[x, \theta] \rho[x, \theta] \sqrt{1 + \frac{u^{(0,1)}[x, \theta]^2}{x^2}} u^{(1,0)}[x, \theta]}{x^2 + u^{(0,1)}[x, \theta]^2} + \frac{x^2 x o^2 \omega^2 v[x, \theta] \rho[x, \theta] \sqrt{1 + \frac{u^{(0,1)}[x, \theta]^2}{x^2}} u^{(1,0)}[x, \theta]}{x^2 + u^{(0,1)}[x, \theta]^2} \\
& \frac{8 \text{ed}^{(0,2)}[x, \theta] u^{(1,0)}[x, \theta]}{h x^2} - \frac{8 \text{ed}^{(1,0)}[x, \theta] u^{(1,0)}[x, \theta]}{h x} + \frac{16 u^{(0,2)}[x, \theta] \text{ed}^{(1,0)}[x, \theta] v^{(1,0)}[x, \theta]}{h x} \\
& \frac{16 \text{ed}^{(1,0)}[x, \theta] u^{(1,0)}[x, \theta] v^{(1,0)}[x, \theta]}{h} - \frac{16 u^{(0,1)}[x, \theta] \text{ed}^{(1,1)}[x, \theta]}{h x^2} + \frac{16 v[x, \theta] u^{(0,1)}[x, \theta] \text{ed}^{(1,1)}[x, \theta]}{h x^2} \\
& \frac{16 v^{(0,1)}[x, \theta] \text{ed}^{(1,0)}[x, \theta] u^{(1,1)}[x, \theta]}{h x} + \frac{16 \text{ed}^{(1,1)}[x, \theta] u^{(1,1)}[x, \theta]}{h x} - \frac{16 v[x, \theta] \text{ed}^{(1,1)}[x, \theta] u^{(1,1)}[x, \theta]}{h x} \\
& \frac{16 \text{ed}^{(1,0)}[x, \theta] u^{(1,2)}[x, \theta]}{h x} + \frac{8 v[x, \theta] u^{(0,2)}[x, \theta] \text{ed}^{(2,0)}[x, \theta]}{h x} + \frac{8 v[x, \theta] u^{(1,0)}[x, \theta] \text{ed}^{(2,0)}[x, \theta]}{h} \\
& \frac{8 v[x, \theta] \text{ed}^{(0,2)}[x, \theta] u^{(2,0)}[x, \theta]}{h x} + \frac{16 \text{ed}^{(1,0)}[x, \theta] u^{(2,0)}[x, \theta]}{h} + \frac{8 v[x, \theta] \text{ed}^{(1,0)}[x, \theta] u^{(2,0)}[x, \theta]}{h} \\
& \frac{3 x^3 \omega^2 \rho[x, \theta] u^{(2,0)}[x, \theta]}{\sqrt{1 + u^{(1,0)}[x, \theta]^2}} - \frac{3 x i^2 \omega^2 \rho[x, \theta] u^{(2,0)}[x, \theta]}{x \sqrt{1 + u^{(1,0)}[x, \theta]^2}} + \frac{3 x x i^2 \omega^2 \rho[x, \theta] u^{(2,0)}[x, \theta]}{\sqrt{1 + u^{(1,0)}[x, \theta]^2}} \\
& \frac{3 x o^2 \omega^2 \rho[x, \theta] u^{(2,0)}[x, \theta]}{x \sqrt{1 + u^{(1,0)}[x, \theta]^2}} + \frac{3 x x o^2 \omega^2 \rho[x, \theta] u^{(2,0)}[x, \theta]}{\sqrt{1 + u^{(1,0)}[x, \theta]^2}} - \frac{x^3 \omega^2 v[x, \theta] \rho[x, \theta] u^{(2,0)}[x, \theta]}{\sqrt{1 + u^{(1,0)}[x, \theta]^2}} \\
& \frac{x i^2 \omega^2 v[x, \theta] \rho[x, \theta] u^{(2,0)}[x, \theta]}{x \sqrt{1 + u^{(1,0)}[x, \theta]^2}} + \frac{x x i^2 \omega^2 v[x, \theta] \rho[x, \theta] u^{(2,0)}[x, \theta]}{\sqrt{1 + u^{(1,0)}[x, \theta]^2}} - \frac{x o^2 \omega^2 v[x, \theta] \rho[x, \theta] u^{(2,0)}[x, \theta]}{x \sqrt{1 + u^{(1,0)}[x, \theta]^2}} \\
& \frac{x x o^2 \omega^2 v[x, \theta] \rho[x, \theta] u^{(2,0)}[x, \theta]}{\sqrt{1 + u^{(1,0)}[x, \theta]^2}} + \frac{8 x \text{ed}^{(2,0)}[x, \theta] u^{(2,0)}[x, \theta]}{h} \\
& \frac{1}{h x^3} \\
& \left. \begin{aligned}
& (16 \text{ed}^{(0,1)}[x, \theta] (-u^{(0,3)}[x, \theta] + u^{(0,1)}[x, \theta] (-1 + v[x, \theta] - x v^{(1,0)}[x, \theta]) - \\
& x (v[x, \theta] u^{(1,1)}[x, \theta] + (-v^{(1,0)}[x, \theta] u^{(1,1)}[x, \theta] + v^{(0,1)}[x, \theta] u^{(2,0)}[x, \theta] + u^{(2,1)}[x, \theta])) + \\
& 16 x \text{ed}^{(1,0)}[x, \theta] u^{(3,0)}[x, \theta]) \\
& h
\end{aligned} \right) \\
& \frac{1}{h x^3} \\
& \left. \begin{aligned}
& (8 \text{ed}[x, \theta] (u^{(0,4)}[x, \theta] + x u^{(1,0)}[x, \theta] + 2 x v^{(0,1)}[x, \theta] u^{(1,1)}[x, \theta] - 2 x^2 u^{(1,1)}[x, \theta] v^{(1,1)}[x, \theta] - \\
& 2 u^{(0,1)}[x, \theta] (v^{(0,1)}[x, \theta] - x v^{(1,1)}[x, \theta]) - 2 x u^{(1,2)}[x, \theta] - x^2 u^{(2,0)}[x, \theta] + x^2 v^{(0,2)}[x, \theta] u^{(2,0)}[x, \theta] + \\
& x^3 v^{(1,0)}[x, \theta] u^{(2,0)}[x, \theta] + x^3 u^{(1,0)}[x, \theta] v^{(2,0)}[x, \theta] + u^{(0,2)}[x, \theta] (4 + x^2 v^{(2,0)}[x, \theta]) + 2 x^2 u^{(2,2)}[x, \theta] + \\
& 2 x^3 u^{(3,0)}[x, \theta] + x^4 u^{(4,0)}[x, \theta]))
\end{aligned} \right)
\end{aligned}$$

The notations used here are as follows:

$$r_i \equiv r_i, r_o \equiv r_o, \nu[r, \theta] \equiv \nu, \rho[r, \theta] \equiv \rho, ed[r, \theta] \equiv D = \frac{Eh^3}{12(1-\nu^2)}, u[r, \theta] \equiv u,$$

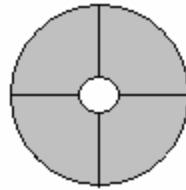
$$\text{and } \xi^{(p,q)}[r, \theta] \equiv \frac{\partial^{(p+q)} \xi}{\partial r^p \partial \theta^q} \text{ where } \xi \text{ is } D, \rho, \nu \text{ or } u \text{ for any } p \text{ and } q.$$

The above result was cross-checked by putting constant values of D, ρ and ν . It gave back the results as in [1] for disk with constant material properties.

The non-trivial solutions to this partial differential equation in r and θ with appropriate boundary conditions give the modal shapes of the rotating disk with inhomogeneous material properties like stiffeners, etc. And the corresponding ω_n 's gives the natural frequencies.

Possibilities of solution. As it can be seen, the obtained differential equation is a pretty huge one and is difficult to handle analytically without any suitable approximations. Attempts were made to reduce the partial differential equation to ordinary ones using separation of variable method. The substitution $u(r, \theta) = u_1(r).u_2(\theta)$ was done, but without much simplification or separation of the variable r and θ . However there are possibilities of further investigation into the equation and solving it analytically using suitable approximation techniques like Galerkin's methods, etc.

However, as the present problem deals mainly with radial stiffeners (*fig-4*), a possible simplification of the equation may be performed by assuming that the properties like D, ρ and ν are functions of θ only.



Disk with 4 stiffeners

fig - 4

Moreover if we assume the stiffeners to be very thin and having drastically different material property values compared to that of the disk itself, the property functions D, ρ and ν may be approximated by a Dirac Delta function as follows:

$$\xi(r, \theta) = \xi_{disk} + \xi_{stiffner} \cdot \delta \left(\prod_{k=-n}^n \left(\theta - \frac{2\pi k}{n} \right) \right),$$

where, ξ is any property of the material integrated over length,

n = number of equispaced stiffeners on the disk.

It may be noted that the domain of θ in which all the analyses are done is assumed to be $[-2\pi, 2\pi]$.

FINITE ELEMENT ANALYSIS

The obtained partial differential equation can be attempted to be solved using suitable numerical techniques. However as a part of the present work, the numerical solutions have been performed using the FEM software Ansys. The description of the geometry, material

properties, boundary conditions, grid type used, meshing and mode extraction method used are given below. All the values mentioned here are in SI unit system.

Geometry of the Disk. The disk was basically a thin annular cylinder with internal radius(r_i) = 0.01, external radius(r_o) = 0.051, thickness(h) = 0.001. The geometry and number of the stiffeners were varied and different sets of results were obtained for each of them.

Material Properties. The material of the disk is considered to be a type of plastic polymer, and the stiffeners were assumed to be made of steel. Hence the material property values were chosen accordingly.

The material of the disk was chosen to have the following properties:

$$E = 40 \times 10^9, \rho = 2000, \nu = 0.25$$

And the material of the stiffener was chosen to have the following properties:

$$E = 200 \times 10^9, \rho = 7800, \nu = 0.3$$

Boundary Conditions. The boundary condition was set so as to ensure that the disk is clamped at its inner circumference. In order to ensure that, the surface area of the inner cylinder of the disk was declared to have zero displacement along all the three degrees of freedom.

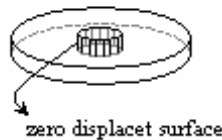


fig - 5

Grid type, meshing and mode extraction technique. For meshing the volume of the disk, the 20-nodes solid element 'SOLID95' provided in Ansys was chosen. The particular choice was made because the SOLID95 element can tolerate irregular shapes without much loss of accuracy and the elements have compatible displacement shapes and are well suited to model curved boundaries. Hence for the present problem dealing with thin circular disk, this element was found to be most suitable.

The meshing of both the disk and the stiffener volumes were done using unstructured grids. For the purpose of controlling the size of the elements Ansys's 'Smart Size' tool was used. For the volumes of the disk, the size level was set to 7 and for the stiffeners the size level was set to 6.

For each case, first a static analysis was performed with the prestressed effect on and with an angular velocity of the global coordinated about z-axis to account for the rotation of the disk. It was followed by a modal analysis with the previously obtained prestress data. For the modal analysis, the method used for extraction of the eigenvalues is Block Lanczos.

The following section describes the geometry, position and number of stiffeners used and the corresponding results obtained in each case.

RESULTS OF FINITE ELEMENT ANALYSIS

The standard mode shapes for disk without stiffeners and clamped at the inner circumference consists of nodal circumferences and nodal diameters. A mode shape with i nodal diameters and j nodal circles is termed as mode (i, j) . The following figures show some typical mode shapes (the lines represent the nodes):

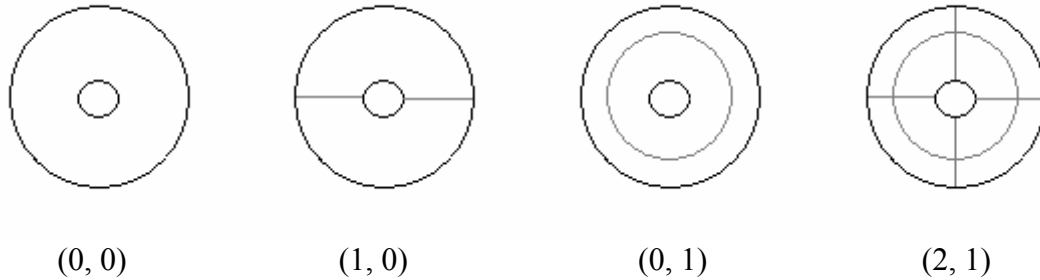


fig - 6

Disk with no stiffeners. Modes obtained: First 20 modes were extracted, and the modal shapes obtained were the standard ones. A plot of the modal frequencies against the angular velocity of the disk is performed. The intersections of the straight lines with slopes 2, 3, etc with curves corresponding to modes (1,0), (2,0), etc give the critical frequencies. The obtained plots being the standard ones haven't been shown in this paper.

It was observed that the slope 1 line almost became asymptotic to the mode (0,0) curve. This is a result expected from the standard calculations for disk with no stiffeners.

Disk with three straight equispaced radial stiffeners

Stiffener Geometry: The stiffeners are simple thin rectangular parallelepipeds with length $r_o - r_i = 0.041$ and both height and thickness = $h = 0.001$.

Modes obtained: The mode shapes obtained were same as before, but for all the modes (i, j) with i as multiple of 3, the frequencies of the orthogonal modes got splitted. The splitted modes are denoted by 'A' for the modes which have stiffeners on antinodes and 'B' for the modes which have stiffeners on modal diameters.

The plot of modal frequencies against the angular velocity is shown in *Graph-1*.

Disk with four straight equispaced radial stiffeners

Stiffener Geometry: Same as *Disk with three straight equispaced radial stiffeners*

Modes obtained: Mode shapes obtained were same as before, but splitting of orthogonal modes was observed for modes with nodal diameters multiples of 4.

The plot of modal frequencies against the angular velocity showed that there hasn't been any significant change in the critical angular velocities.

It may be observed here that till now there has not been any significant change in the critical angular velocities because of addition of stiffeners to the disk. Hence an investigation by altering the geometry of the stiffeners may be done to see if the critical angular velocities go up. The following sections show the results obtained by altering the stiffener geometries.

Disk with three expanding (narrower near the inner circumference, wider near the outer circumference) equispaced radial stiffeners.

Stiffener Geometry: The stiffeners are trapezoidal shaped thin blocks with width of 0.0004 at the inner circumference and 0.002 at the outer circumference.

The thickness is uniform thought and is equal to $h = 0.001$.

On starting the analysis with zero angular velocity of the disk, it was found that the modal frequencies, and hence the critical speeds decreased considerably compared to the straight stiffeners case. This as the undesired case, hence further continuation of analysis with this geometry of stiffener was discontinued.

However it was clear from the above mentioned observation that an increased mass concentration near the outer circumference is not desirable. Hence it may be interesting to do some study with stiffeners having higher mass concentration near the inner circumference.

Disk with three contracting (wider near the inner circumference, narrower near the outer circumference) equispaced radial stiffeners

Stiffener Geometry: As in 5.4, the stiffeners are the same trapezoidal shaped thin blocks, but they are now placed in a reverse orientation. That is, they have a width of 0.0004 at the outer circumference and 0.002 at the inner circumference.

The thickness is uniform thought and is equal to $h = 0.001$.

Modes obtained: Mode shapes obtained were similar to 5.2, with splitted orthogonal modes for modes with nodal diameters multiples of 3. However in this case, a few modes were found to be slightly deformed from the standard mode shapes. The modal frequencies vs. angular velocity plot is shown in *Graph-2*.

Intermediate Conclusions for proceeding with further modifications on the stiffener geometry. Though not very evident from the previous graphs, there had been a minor increase in the critical frequencies with contracting stiffeners when compared with the previous ones. A close comparative study of the frequencies of mode (1, 0) and its intersection with slope 2 line may reveal the fact (refer to the plot *graph-3*).

The *graph-3* reveals:

- With addition of stiffeners, the lowest critical velocity has gone up slightly.
- By increasing the number of stiffeners from 3 to 4 not much difference id made on the critical velocities.
- By increasing the mass concentration of the stiffeners near the inner circumference there has been some increase in the critical velocity.
- However, in all the above mentioned cases the value of the first critical angular velocity lies within the value 1500 (± 50) rad/s. Hence nothing much has yet been achieved. Hence further investigation is required

From the above drawn conclusions it was logical to investigate the problem with stiffeners having even higher mass concentration near the inner circumference. The following section deals with such a stiffener geometry, which is a modification on the contracting stiffener, and was found to give much better results.

Disk with three raised, contracting (raised above the surface of the disk and wider near the inner circumference) equispaced radial stiffeners

Stiffener Geometry: The stiffeners are the similar to those of section 5.5, but they are now also raised above the surface of the disk near the inner circumference and gradually slopes down to meet the disk surface at the outer circumference. Hence, they are a sort of truncated

pyramidal shaped stiffeners with the base of the pyramid at the inner circumference, and apex at the outer circumference. At the inner circumference they have a width of 0.002 and thickness of 0.00512. And at the outer circumference they have a width of 0.0004 and thickness of 0.001. Thus the geometry appears as shown in the following figure (figure not to the scale):

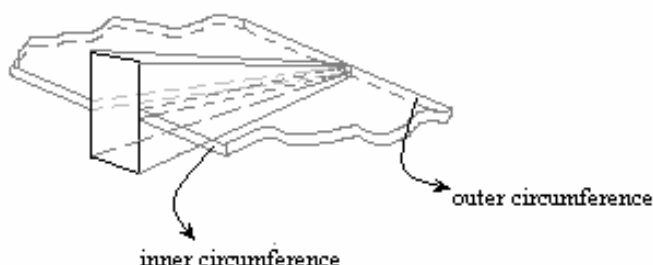


fig – 7

Modes obtained: In this case the mode shapes obtained were rather very interesting. Apart from a few standard higher mode shapes (like (4,0), (5,0), (6,0) and (3,1)), a few new types of modes were obtained, some of which were much deformed an asymmetric.

It was interesting to observe that the standard modes with the lower modal frequencies were completely replaced by new modes with much higher modal frequencies. Hence the first few critical speeds of the disk were expected to increase considerably.

Only a few of the standard modes were available, and they are shown in *graph-4*.

But it will be of greater interest to make a study on the new mode shapes obtained with the present stiffener geometry. The following figures show some of those mode shapes:

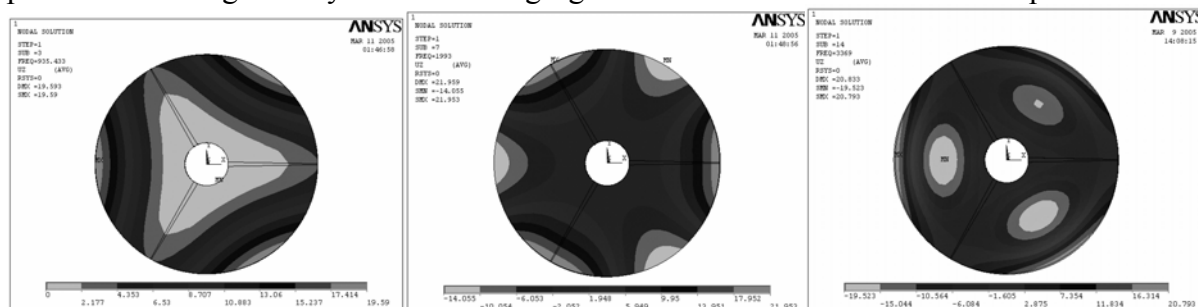


fig – 8 : Unusual mode shapes obtained

As most of the standard (i, j) modes are absent with the present stiffener geometry, we will term the modes mode-1, mode-2, etc. in ascending order of their modal frequencies. For the purpose of comparison with the other stiffener geometries the modal frequency vs. angular velocity graphs were plotted for the different stiffeners for mode-1, mode-2 and mode-3. The plots are given in *graph - 5, 6 and 7*.

From the *graphs 5, 6 and 7* it can easily be seen how the 3 contracting and raised stiffeners used in this section have increased the modal frequencies for the disk substantially.

However, as many of the standard modes were absent, it is difficult to draw any immediate conclusions regarding the critical speed of the disk. But as the modal frequencies were found to increase considerably, one can logically expect the critical velocities to increase accordingly.

Hence the raised contracting stiffener gave extremely desirable results by increasing the modal frequencies. Even if we keep some allowance in these results in order to account for the numerical errors caused due to difference in meshing, the results show a high potential for the success of the stiffener geometry mentioned in this sub-section.

However some of the mode shapes obtained in the simulation with this stiffener geometry were highly deformed and asymmetric. This may be because of numerical errors caused by uneven meshing, limitations of the mode extraction and solving methods used, etc. Further investigation is possible in order to explain these anomalous modal shapes.

CONCLUSIONS

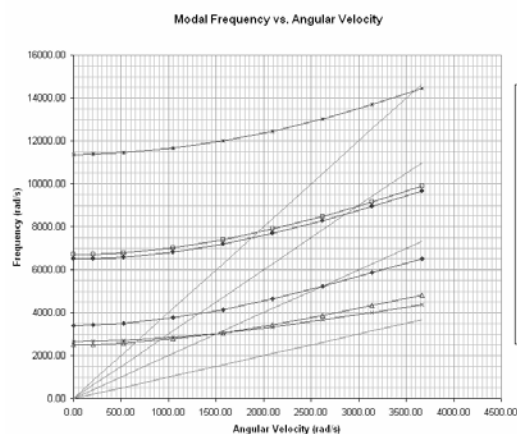
The final conclusions that can be drawn from the above analysis and results:

- An analytical solution has been attempted in order to account for variation of material properties within the disk, which is in fact the case for disks with stiffeners. A differential equation has been successfully set up and cross-checked by putting constant values of material properties to obtain the equation in [1]. However a final solution could not be achieved at the present moment due to the complexity of the differential equation. Further studies on the obtained partial differential equation with appropriate approximations may lead to a satisfactory analytical solution.
- Using the FEM software Ansys, modal analysis of the rotating disk with stiffeners of different geometries were performed. A gradual development of the stiffener geometries on the basis of conclusions drawn from intermediate results finally yielded a stiffener which could successfully push up the modal frequencies, and hence potentially increase the critical speeds of the disk.
- Further investigation into the problem may result in a successful analytical method for dealing with such disks with stiffeners. Moreover variation in the dimensions and geometry of the obtained stiffener may yield better and interesting results.

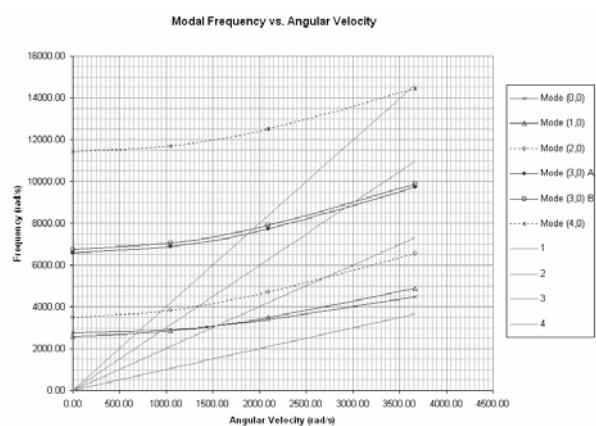
ACKNOWLEDGEMENT

I would like to thank Prof. Anirvan Dasgupta, Dept. Mechanical Engineering, IIT Kharagpur for his invaluable suggestions and help that made it possible for me to complete this particular work successfully.

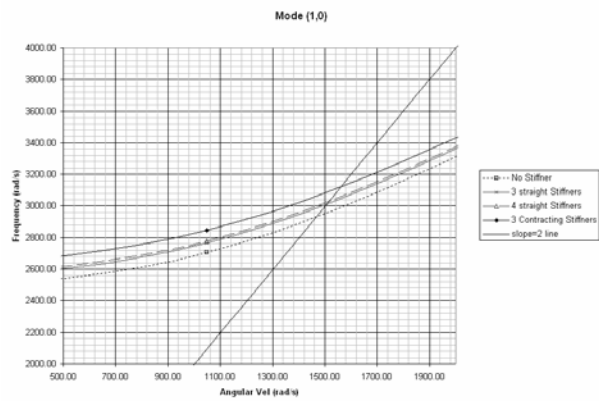
GRAPHS



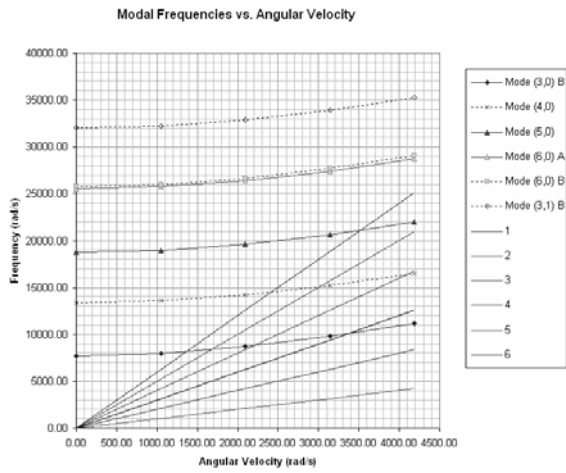
graph -1



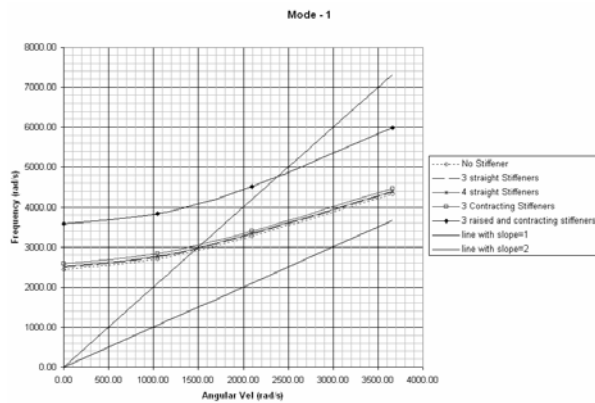
graph -2



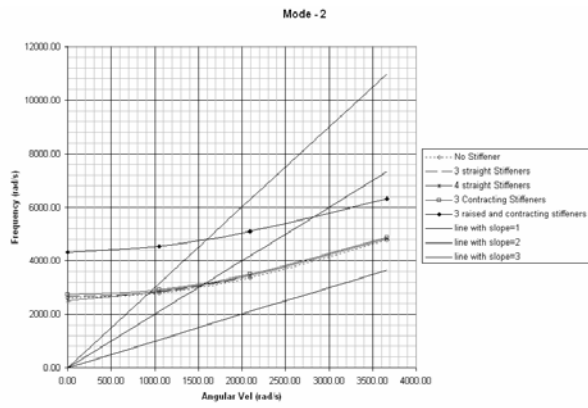
graph -3



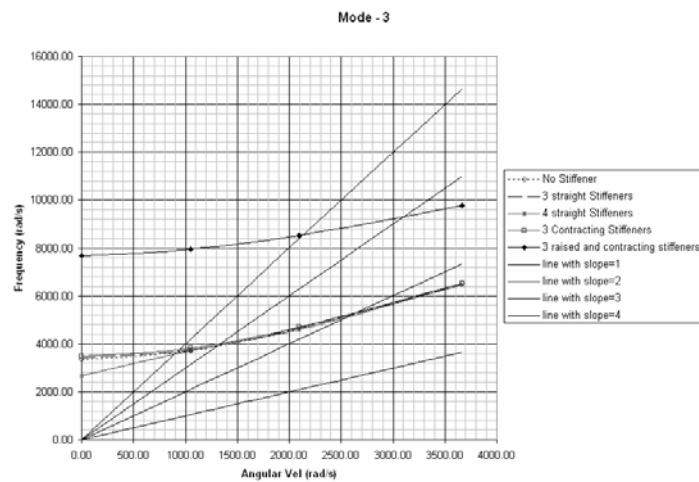
graph -4



graph -5



graph -6



graph -7

REFERENCES

1. S.Timoshenko and S.W.Krieger, *Theory of Plates and Shells*, Prentice Hall.
2. Egor Popov, (1973), *Introduction to Mechanics of Solids*, Delhi, Printice Hall.
3. Erwin Kreyszig, *Advanced Engineering Mathematics*, John Wiley & Sons Inc.